VOL. 18, NO. 13, JULY 2023 ISSN 1819-6608
ARPN Journal of Engineering and Applied Sciences

www.arpnjournals.com

GREEN SYNTHESIS AND CHARACTERIZATION OF MAGNESIUM OXIDE NANOPARTICLES FOR GAS SENSOR APPLICATION

Siraj R. Kareem and Najwa J. Jubier
Department of Physics, Collage of Science, University of Wasit, Iraq
E-Mail: iraqadam33331@gmail.com

ABSTRACT

Green approach synthesis to produce metal oxide nanoparticles (MgO NPs) is so important due to unique properties controlled by the synergistic effects of metal and plant-constituents using plant extracts of Chickpea leaves plant have been effectively as a natural and renewable reducing, chelating, stabilizing, natural binding agent, and precipitating agent, it is used in the synthesis of magnesium oxide nanoparticles. The synthesized MgO nanoparticles have a cubic crystal structure with an average crystallite size of (22.08nm) at 800 nm, according to the X-ray diffraction (XRD) pattern. The synthesized MgO nanoparticles have a cubic crystal structure with an average crystallite size of (22.08nm) and, (EDX Spectrum) shows the composition of MgO. FE-SEM characterization revealed the presence of MgO with a spherical shape, and the average particle size was confirmed (31.23 nm). As indicated by the anisotropic patterns of MgO, the obtained (Raman) spectrum of MgO shows a strong peak in different regions indicating the cubic structure. The optical energy gap was calculated using DRS analysis and found to be (4.8eV). Gas sensing tests for H_2S and NO_2 revealed that these hierarchically porous MgO architectures were highly promising for gas sensor applications. Their unique structures significantly improve gas diffusion in the material.

Keywords: green synthesis, magnesium oxide, gas sensor.

Manuscript Received 7 March 2023; Revised 28 August 2023; Published 13 September 2023

1. INTRODUCTION

Nanoparticles have received a lot of attention in recent years due to their unique physicochemical properties, such as high strength with good thermal conductivity, high damping properties, and mechanical stability. [1]. Because of their wide range of applications, nanoscale metals and metal oxides have ushered in a new era of materials in materials chemistry. [2]. MgO is a significant inorganic oxide and one of the most important metal oxides with numerous applications due to its high surface reactivity, and chemical and thermal stability in sensors, catalytic coatings, and so on. [3, 4]Magnesium oxide nanoparticles and microparticles are commonly used as reinforcing reagents in the superconducting industry [5]. MgO nanoparticles are grown using a variety of fabrication techniques that require high-temperature, sophisticated, and/or expensive tools. [6]. As a result, the biosynthetic pathway (green synthetic processes) has emerged as a promising candidate for large-scale synthesis and production of nanostructured materials and magnesium oxide. The green synthesis (using a chickpea plant) and characterization of cubic crystalline structure MgO nanoparticles were described in this paper. [7].

2. EXPERIMENTAL PART

Magnesium oxide nanoparticles were synthesized using magnesium nitrate ($MgNO_3.6H_2O$) as a source. All of the chemical materials used were purchased from Aldrich Chemical. Have been used (1g) of magnesium nitrate ($MgNO_3.6H_2O$) was dissolved in (30 ml) of deionized water, (and 25 ml) of chickpea plant extract, Add the solution dropwise into the prepared magnesium nitrate solution with continuous stirring in a magnetic mixer. After a few minutes of stirring, a white precipitate of magnesium hydroxide appeared in the beaker and remained for (15) minutes. The pH of the solutions was measured (11). The precipitate was filtered using centrifuged and left at R.T. Then the dried samples were Calcined thermally for (2) hours at (800°C and 250°C) were done. After that, the magnesium oxide thin films were prepared for use in the gas sensor application. This was done by mixing the prepared nanomaterials (magnesium oxide) with (1 g) of synthetic polymer material PVA and (20) ml of deionized water and mixing them in a magnetic mixer under (80 °C) for (10) minutes, it was placing them on glass bases after washing well and burning in the oven at (450°C) for two hours and send to the test of sensitivity to NO_2 and H_2S.

3. CHARACTERIZATION

Field emission scanning electron microscopy was used to perform the morphological examination (FE-SEM). A diffractometer (XRD) was used to determine crystallinity and other techniques like RAMAN and DRS to measurements of the absorption coefficient and the energy gap was also taken through the (DRS) test. Finally, testing sensitivity tests and finding out the response and recovery times for the prepared samples.

4. RESULTS AND DISCUSSIONS

4.1 X-Ray Diffraction Result

X-ray diffraction was used to identify the crystal structure of MgO nanoparticles and interplanar distance. The average crystalline size was determined using the Debye–Scherer equation:

$$D = \frac{0.9\,\lambda}{\beta \cos\theta} \quad (1)$$

D, is the crystallite size (nm), λ, is the X-ray wavelength, θ is, the Bragg diffraction angle, and β is (FWHM). Equation (2) is used to measure the inter-planar distance (d) [8].

$$n\lambda = 2dsin\theta \quad (2)$$

Figure-1 depicts the X.R.D patterns for MgO NPs at R.T and 800° C. It was demonstrated that there are three sharp peaks and 2 θ. It was observing diffraction peaks at (001), (101)(102), (110), (111), (200), (303), and (222) and at 800 ℃ with (111), (200), (202) and (222) diffraction planes respectively, results were agreeing and matched with standard ICCD file no, (96-100-0055) and (96-900-6748) respectively. It was found that the results showed the prepared nano MgO are cubic structure with polycrystalline, and the crystallinity was calculated using FWHM values (full width at half maximum) by using the Scherrer equation, the crystal size of magnesium nanoparticles prepared at R.T and 800 ℃ was calculated and based on Miller coefficients, where the average crystal size appeared to be (14.49nm) and (22.08 nm) respectively, as shown in Tables (1 and 2). This indicates that the crystalline size of the particles increased with increasing temperature. MgO was found to have high purity and crystallinity preparing at 800 ℃ [9].

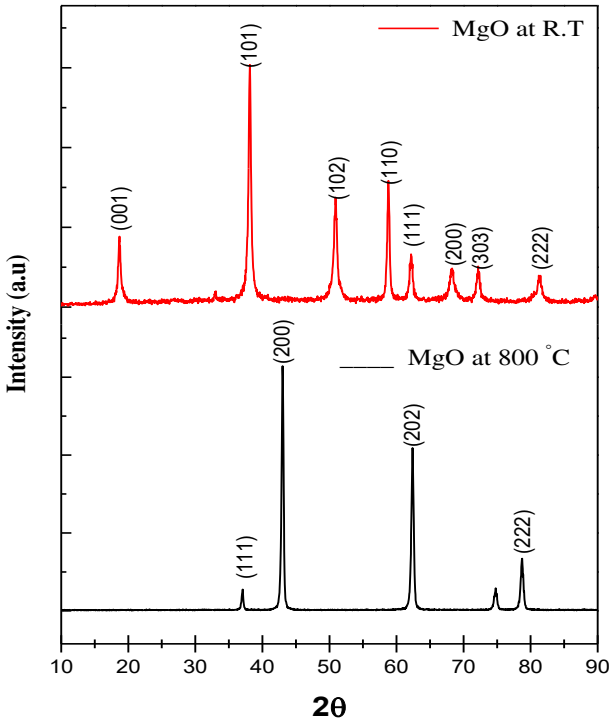

Figure-1. XRD patterns of MgO NPs at R.T and 800 ℃.

Table-1. Structural properties of MgO NPs at R.T.

2θ (Deg.)	FWHM (Deg.)	dhkl Std.(Å)	dhkl Exp.(Å)	Crystallite size (nm)	Average crystallite size (nm)
18.68	0.52	4.81	4.75	15.54	14.49
38.12	0.54	2.60	2.36	15.65	
50.90	0.72	1.48	1.79	12.23	
58.79	0.45	1.91	1.57	20.24	
62.18	0.60	1.46	1.49	15.38	
68.27	0.96	1.48	1.37	9.96	
72.18	0.66	1.38	1.31	14.81	
81.31	0.87	1.36	1.18	12.08	

Table-2. Structural properties of MgO NPs at 800 ℃.

2θ (Deg.)	FWHM (Deg.)	dhkl Std.(Å)	dhkl Exp.(Å)	Crystallite size (nm)	Average crystallite size (nm)
37.03	0.33	2.53	2.43	25.06	22.08
43.01	0.37	2.16	2.10	23.14	
62.39	0.44	1.50	1.49	20.96	
74.77	0.54	1.30	1.27	18.55	
78.72	0.51	1.6	1.21	20.24	

4.2 Scanning Electron Microscope (SEM)

The morphological and crystallographic details of the magnesium oxide nanoparticles obtained were examined using FE-SEM. Figure-2 depicts the morphology of nano MgO specimens calcined at (800°C) temperature using different magnification (FE-SEM) images. The scanning images revealed that the green method samples contained spherical particles and a uniform distribution of particles with an average particle size (31.23 nm). These findings are comparable to previous findings for MgO synthesis. [10, 11].

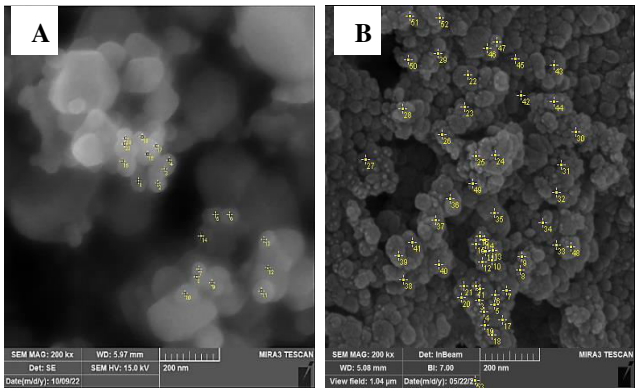

Figure-2. FE-SEM images show the surface morphology of the MgO NPs at 800 ℃ with different magnifications (a) 200 nm, (b) 500 nm.

The EDX Spectra used to validate the production of MgO NPs are shown in Figure-3. The EDX spectrum's Mg K and O k emission series peaks confirmed the stoichiometry of the synthesized NPs. The magnesium and oxygen elements in the specimen had a close stoichiometric ratio. The quantitative results of the weak and robust absorption peaks in the Mg and oxygen regions are given in the graph's Table, and these results are consistent [13]. It also provides the element's normalized concentration in weight percentage (W%) and atomic weight percentage (A%) for Mg and oxygen. As illustrated in the attached table with Figure-3.

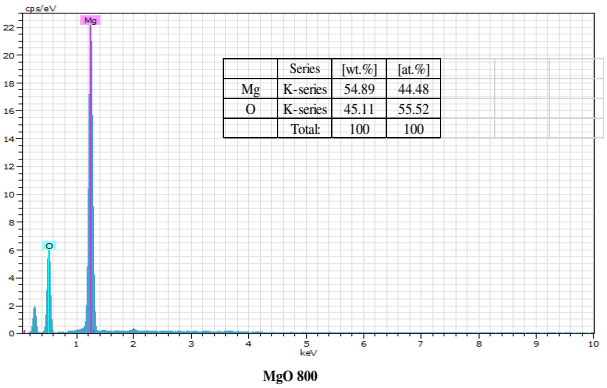

	Series	[wt.%]	[at.%]
Mg	K-series	54.89	44.48
O	K-series	45.11	55.52
	Total:	100	100

Figure-3. The EDX Spectrum for MgO NPs.

4.3 Raman Scattering Result

As shown in Figure-4, The Raman scattering in MgO at 800°C with particle size is observed (nm). It was discovered that the second-order Raman lines in MgO nanocrystals vanish in all microcrystals, while new peaks emerge at 1462.74, 2849.50, and 3698.15 cm1. Because first-order Raman scattering is forbidden in bulk crystals, Raman lines with lower frequencies are discussed, which are enhanced as particle size decreases. The assignment is supported by the photon density of states in microcrystals. Peaks lower than 1500 cm-1 are associated with D-band, also known as breathing mode. A G-band is represented by the peaks at 1500 cm-1 and 3000 cm-1. The indirect measurement of crystallite size and defects is correlated with the ratio of (D and G) band intensities, or ID/IG. The reported data shows that this data is consistent. [12] The Raman spectrum of nano MgO reveals the presence of a strong peak in various regions, indicating the cubic structure as designated to the tangential modes of MgO in the amorphous phase. Complex absorption bands were observed in the (2500 - 4000) cm^{-1} region, which corresponds to the frequency of oxygen l ion stretching. The crystal structure with its single formula unit per primitive unit cell leads to the prediction of only one infrared active hydroxyl stretching mode [13].

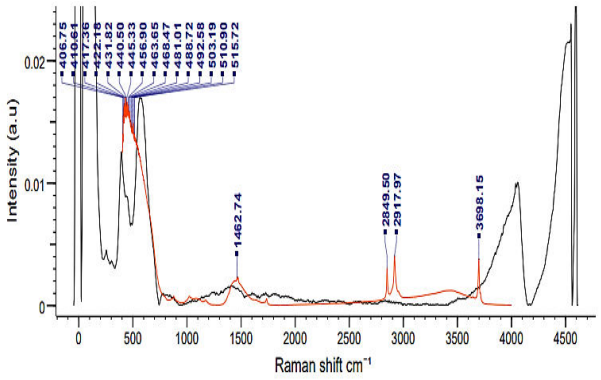

Figure-4. Raman spectrum of Nano MgO at 800℃

4.4 DRS Analysis

Figure-5 shows a chart of the absorbance spectrum curve of the prepared MgO sample as a function of wavelength at 800℃, as it was found that the material has high absorbance at short wavelengths that indicate Short wavelengths and high energies relative to the wavelength, and this is a unique property that characterizes nano-sized materials, as the field of work will be the absorbance in applications under visible light and within the field of ultraviolet rays upwards [14, 15]

Also, through DRS analysis, the optical energy gap was calculated using the (Tauc) method from equation (3), which can be written after setting the value of the constant equal to the value (1⁄2) in the following form:

$$(\alpha h\nu)^2 = (\alpha E)^2 = B^2(h\nu - E_g) \quad (3)$$

From drawing the graphic relationship between $(\alpha h\nu)^2$ and the photon energy ($h\nu$), The energy gap, or permitted transition at the point, is determined by extending the straight portion of the curve to cut the photon energy axis. $(\alpha h\nu)^2 = 0$ as shown in the Figure-5, where it appeared worth approximate (4.8eV).

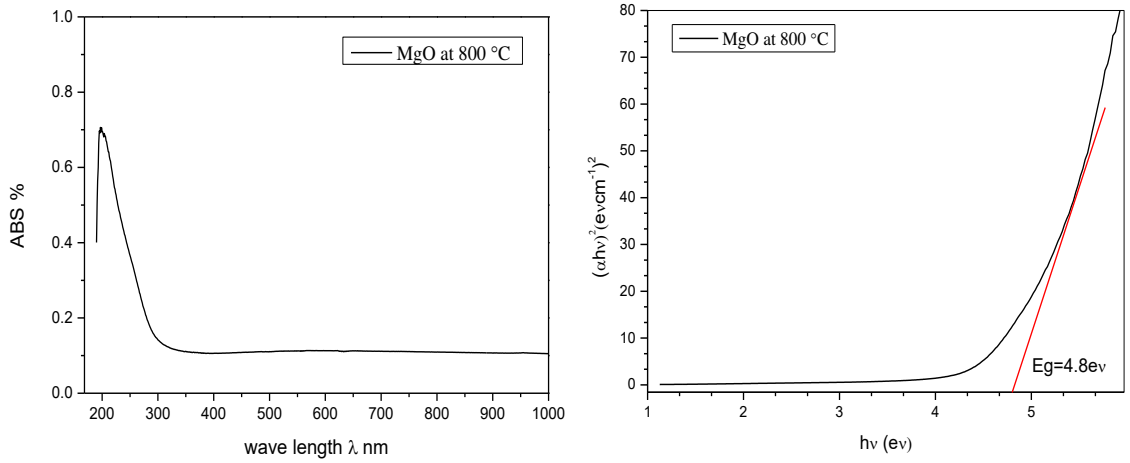

Figure-5. Absorbance spectrum and energy gap for MgO at 800℃.

4.5 Gas Sensor Measurements

The prepared nanomaterials were deposited on glass bases to form thin films to be used in the application of a sensor once for an oxidizing gas and another for a reducing gas, namely NO_2, and H_2S Gas. The sensitivity of the studied gases appeared affected by the high temperature, as shown in Figure-6, where with NO_2 gas, it is clear that the sensitivity is constant at first, then a decrease occurs at approximately (240 ℃), and then the rise returns. As for H_2S gas, it was noted that the onset of sensitivity was less, but with a temperature rise it increased, and then a decrease occurred at (240 °C), after which the rise returned, and this indicates that the temperature has a major and major effect on the work of the sensor, as impurities and secondary gases are expelled that affect the response of the sensor in the beginning.

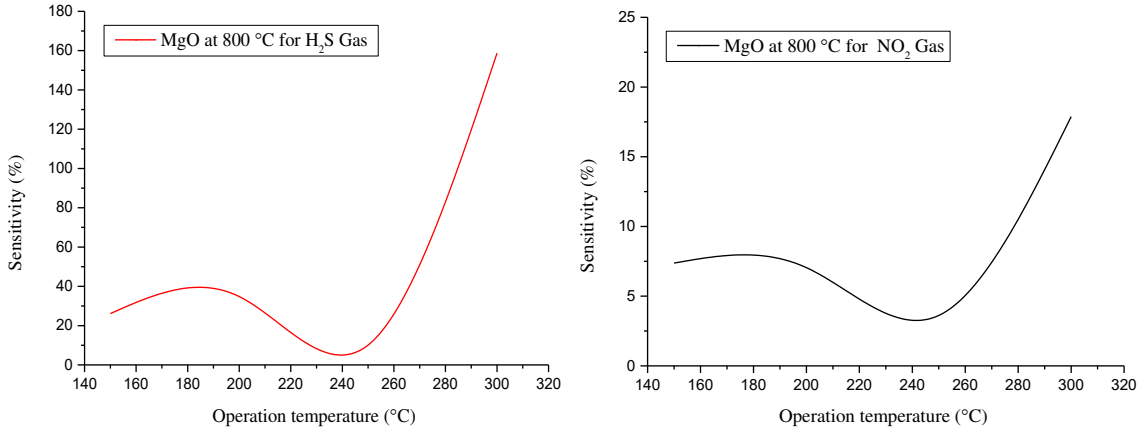

Figure-6. Shows Operation temperature effect on sensing properties for MgO NPs.

The response time and recovery time for the NO_2 gas sensor were also calculated, and the result was an increase in the response time with the rise in temperature until it reached a peak, and then a decrease. As for the recovery time, it was constantly decreasing with the rise in temperature until it reached a certain level, and then a rise occurred due to the highly promising, gas diffusion and mass transportation in sensing materials according to their unique properties. The same is true for H_2S gas, as shown in Figure-7, the sensor's response time gradually decreased and then increased as temperature rose, whereas the recovery time initially increased gradually before falling off at a certain point before rising again.

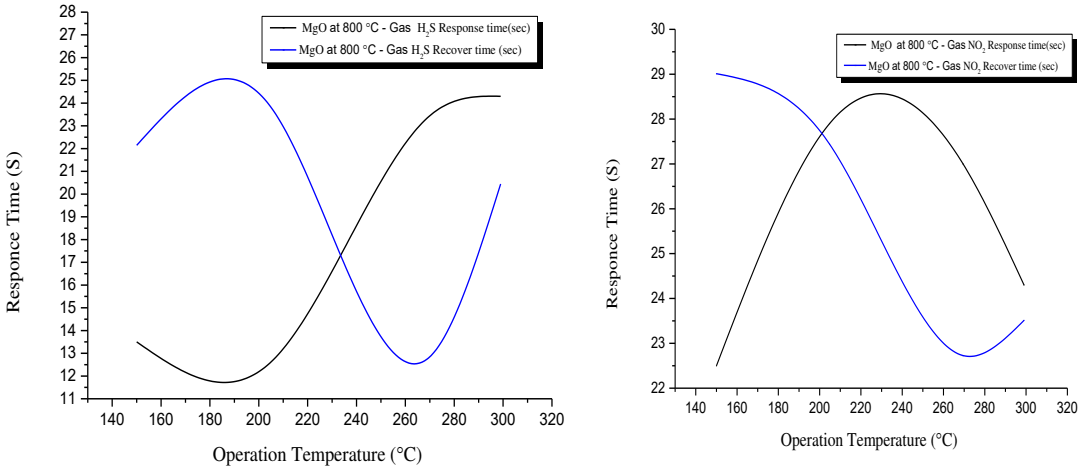

Figure-7. Shows the Response time and recovery time for the sensor used.

5. CONCLUSIONS

The biosynthesis of magnesium oxide nanoparticles has been successfully synthesized in environmentally friendly, appropriate quantities using chickpea plant extract as a natural binding agent that acts as an oxidizing agent in the chemical reaction. The crystal structure obtained by XRD, the cubic structure of magnesium oxide, and the FE-SEM spherical structure of the growth of magnesium oxide nanoparticles and show that further high-temperature annealing increases the arrangement of the particles. The spherical shape possessed by the magnesium oxide nanoparticles with a high surface area acts as a very good reducing agent and is considered a natural, renewable, low-cost, and effective bio for the synthesis of magnesium oxide nanoparticles. It is then used in critical applications such as gas sensors operating at relatively high temperatures

ACKNOWLEDGEMENTS

The authors would like to thank the Department of Physics, College of Science, University of Wasit, Iraq, for supporting this work.

REFERENCES

[1] Gray J. and Luan B. 2002. Protective coatings on magnesium and its alloys-a critical review Journal of alloys and compounds. 336: 88-113.

[2] Chen J., Feng J. and Yan W. 2016. Influence of metal oxides on the adsorption characteristics of PPy/metal oxides for Methylene Blue Journal of colloid and interface science. 475: 26-35.

[3] Wahab R., Ansari S., Dar M. A., Kim Y. S. and Shin H. S. 2007. Synthesis of magnesium oxide nanoparticles by sol-gel process. In: Materials Science Forum: Trans Tech Publ) pp. 983-6.

[4] Shukla S., Parashar G., Mishra A., Misra P., Yadav B., Shukla R., Bali L. and Dubey G. 2004. Nano-like magnesium oxide films and its significance in optical fiber humidity sensor Sensors and Actuators B: Chemical. 98: 5-11.

[5] Richards R., Li W., Decker S., Davidson C., Koper O., Zaikovski V., Volodin A., Rieker T. and Klabunde K. J. 2000. Consolidation of metal oxide nanocrystals. Reactive pellets with controllable pore structure that represent a new family of porous, inorganic materials Journal of the American Chemical Society. 122: 4921-5.

[6] Bruley J., Stemmer S., Ernst F., Rühle M., Hsu W. Y. and Raj R. 1994. Nanostructure and chemistry of a (100) MgO/(100) GaAs interface Applied physics letters. 65: 564-6.

[7] Yang P. and Lieber C. M. 1996. Nanorod-superconductor composites: a pathway to materials with high critical current densities Science. 273: 1836-40.

[8] Thamir A. A., Jubier N. J. and Odah J. F. 2021. Antimicrobial activity of zirconium oxide nanoparticles prepared by the sol-gel method. In: Journal of Physics: Conference Series: IOP Publishing). p. 012058.

[9] Dobrucka R. 2018. Synthesis of MgO nanoparticles using Artemisia abrotanum herba extract and their antioxidant and photocatalytic properties Iranian Journal of Science and Technology, Transactions A: Science 42 547-55

[10] Ramanujam K. and Sundrarajan M. 2014. Antibacterial effects of biosynthesized MgO

nanoparticles using ethanolic fruit extract of Emblica officinalis Journal of photochemistry and photobiology B: biology. 141: 296-300.

[11] Yuvakkumar R. and Hong S. I. 2014. Green synthesis of spinel magnetite iron oxide nanoparticles. In: Advanced Materials Research: Trans Tech Publ) pp. 39-42.

[12] Liu B., Yu B. and Zhang M. 2005. Catalytic CVD synthesis of double-walled carbon nanotubes with a narrow distribution of diameters over Fe-Co/MgO catalyst Chemical Physics Letters 407 232-5.

[13] R. Soniya S. and Nair V. M. 2016. Synthesis and characterization of nanostructured Mg (OH) 2 and MgO International Journal of Science and Research (IJSR) 5: 199-203.

[14] Jayachandran A., Aswathy T. and Nair A. S. 2021. Green synthesis and characterization of zinc oxide nanoparticles using Cayratia pedata leaf extract Biochemistry and Biophysics Reports 26 100995

[15] Silva A. A., Sousa A. M. F., Furtado C. R. and Carvalho N. M. 2022. Green magnesium oxide prepared by plant extracts: synthesis, properties and applications Materials Today Sustainability 100203